

Received: 13 February 2019 • Accepted: 15 July 2019

Research

doi: 10.22034/jcema.2019.208084.1010

Probabilistic Analysis of Bearing Capacity of Strip Foundations Overlying Reinforced Embankments

Shayan Bayat, Ali Sanaeirad*

Department of Civil Engineering, Arak University, Arak, Iran

* Correspondence should be addressed to Ali Sanaeirad, Department of Civil Engineering, Cucas University, Arak, Iran Tel: +9183614708; Fax: +982166778905 Email: a-sanaei@araku.ac.ir

ABSTRACT

In cases where the soil underlying the foundation is loose and unable to carry the loads imposed by the structure, improving the soil by an appropriate approach is essential. The application of polymeric materials such as geogrids, in recent decades, has been of interest to engineers and researchers in order to increase the bearing capacity of soil foundations. Geogrid reinforcements allow for achieving an increased bearing capacity or a reduced layer thickness of soil improvements. The most significant factor used in the design of shallow foundations is the bearing capacity of the foundation along with its settlement. In geotechnical investigations, probabilistic analyses could be beneficial in the relevant problems. The Monte Carlo probabilistic simulation method is one of the most commonly used methods in solving geotechnical problems. Therefore, in the current research, a reasonable estimation of the bearing capacity of a strip foundation has been conducted by using a numerical model with the help of the discrete-element software FLAC3D in conjunction with the calculation of the probabilistic bearing capacity via the Monte Carlo simulation method and by considering the uncertainty of the soil internal friction angle and cohesion coefficients.

Keywords: Bearing capacity; strip foundation; reinforced embankment, numerical modeling, Monte Carlo

Copyright © 2019 Ali Sanaeirad. This is an open access paper distributed under the [Creative Commons Attribution License](https://creativecommons.org/licenses/by/4.0/). Journal of Civil Engineering and Materials Application is published by *Pendar pub*; Journal p-ISSN 2676-232X; Journal e-ISSN 2588-2880.

1. INTRODUCTION

On account of the weakness of soils against tensile stresses, designers have constantly been seeking the best solution to obviate this shortcoming. As a result, the tensile and shear strength of soils are expected to be improved by reinforcing the soil. Reinforced soil slopes are among the structures that benefit from this technique. With the advancements in polymer engineering & sciences in recent decades, geosynthetics – which possess superior advantages over other reinforcements – have been introduced as a suitable option to reinforce the soil. Alternatively, the application of a broad range of soils in combination with their easy execution technique has turned the reinforced soil into an economical option in civil projects [1]. Calculating the bearing capacity of strip foundations is an important and common task, the suitable estimate of which is requisite for a sound and safe design. The traditional techniques of calculation of the bearing capacity of foundations do not consider the uncertainty. One of the most substantial issues in the design and application of all types of foundations is to determine the bearing capacity, which was introduced, for the first time, by Terzaghi in 1948 [2], after which it was developed by other researchers throughout different periods of time. It has been nearly 40 years as of the recognition of the reinforcements as useful products in civil and geotechnical projects, during which they have been

utilized in many projects, and their applications and production growth rate have been rapid [3-7]. Due to the recent advances in the polymer industry, the development of geosynthetics has also acquired a much faster rate. The term “geosynthetic” is used for a set of products that are generally applied in order to resolve the geotechnical problems [8]. Geosynthetics increase the bearing capacity of foundations, and protect retaining walls, asphalt pavements, drainage systems, hydraulic structures, etc. from erosion [9-12]. Most of the design methods of reinforced structures are based upon the limit equilibrium method by assuming the location and mechanism of failure. Moreover, it is assumed in this method that the failure mechanism is similar to the reinforced soil, which has been suggested by Terzaghi, as well as that the effect of the reinforcement is applied as a tensile strength in the design calculations. This idea has been employed by many researchers [13]. And Hull et al. [14], in the studies accomplished on reinforced embankments and slopes. These researchers utilized a simple computational method, and supposed that it is possible to consider the behavior of soils and reinforcements independently. However, there is an interaction between a soil and its reinforcement, and it appears that the failure mechanism of reinforced soils occurs gradually owing to the tensile properties of reinforcements. In a research which that was

performed by Hang et al. to determine the accurate failure mechanism directly, a method has been used to predict the bearing capacity of a sand reinforced by tensile materials placed exactly horizontally underneath the foundation [15]. Malkawi et al. investigated the bearing capacity of shallow foundations overlying reinforced soils, resulting in a design methodology [16]. Guido et al. examined the influence of various parameters on the bearing capacity of a geogrid-reinforced sand. After having investigated the outputs, they found that the number of geogrid layers, geogrid width and the first interval of the geogrid layer from a reference point require optimization to achieve the most bearing capacity [17]. Numerous researches regarding the reinforcement of sand by reinforcing strips and geosynthetics have proven the reinforced sand to increase the bearing capacity and decrease the settlement significantly [17-21]. Hegde and Sitharam carried out their analysis on a foundation overlying a clay by means

of a probabilistic approach called the Monte Carlo method, resulting in the fact that the probability of the foundation failure under vertical loads is more plausible [22]. Cerato et al. indicated the spatial variability mechanism of a clay subject to the combined loading on the foundation [23]. Seun Park and Dohi used an elastoplastic behavior to model the soil according to the Mohr-Coulomb (MC) failure criterion for sand and clay. In comparison with the contemporary theoretical relationships, these equations are more accurate as well as consider the interlayer strength, which is reliable [24]. In this research, a rational estimate of the bearing capacity has been completed using numerical modeling via the discrete-element software FLAC3D; and calculating the probabilistic bearing capacity has been carried out by using the Monte Carlo simulation method along with considering the uncertainty of the soil internal friction angle and cohesion parameters.

2. MATERIALS AND METHODOLOGY

2.1. CONSTITUTIVE MODEL AND FAILURE CRITERION

The Mohr-Coulomb (MC) constitutive model has been used to model the soil as it is capable of modeling the soil plastic behavior in case the displacements exceed the elastic limit.

2.2. STRUCTURAL ELEMENTS

2.2.1. GEOGRID

A geogrid reinforcing element has been utilized in order to model the slope reinforcement. Fig. 1 displays the coordinate system of the geogrid structural element.

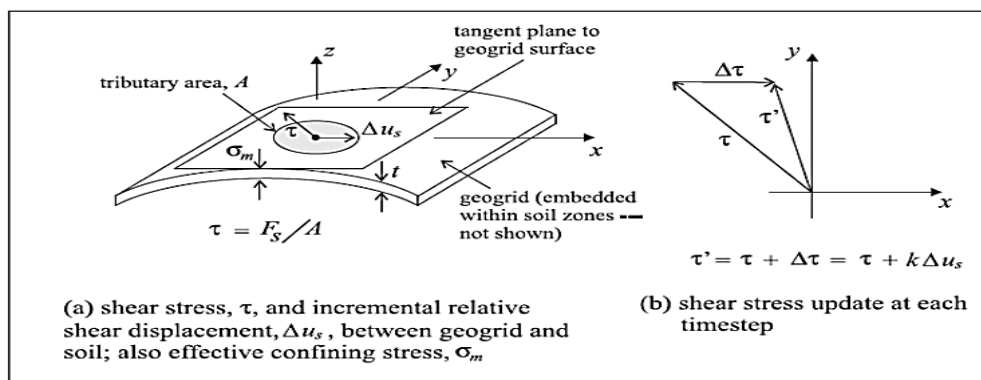


Figure 1. The coordinate system of geogrid structural element

The shear behavior on the surface of the element and the grid includes cohesive strength and internal friction angle.

The shear behavior of the geogrid element is shown in Fig. 2.

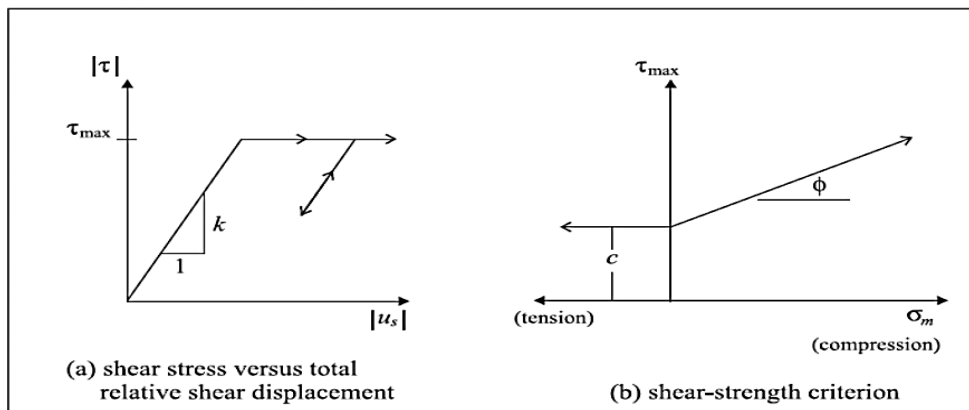


Figure 2. Shear behavior of geogrid element

2.2.2. SHELL STRUCTURAL ELEMENT

A shell element with 18 degrees of freedom is used in order to model the head of the foundation, Fig. 3.

2.3. MODEL GEOMETRY

Before to applying the loading on the strip foundation, initially, the model should be solved statically. The loading analysis is performed after investigating and ensuring the validity of the static analysis results. In the case of the static analysis, the model boundaries are fixed, meaning that the model movement is constrained in each

of the three directions for its base and in the horizontal direction for its side boundaries (only perpendicular to these boundaries), respectively. It should be mentioned that the upper model boundary is free because of the movements in the natural ground surface, for which defining a boundary condition is not necessary. Before exerting the loading on the foundation, the model should reach an initial equilibrium by using the gravitational acceleration; and the maximum unbalanced force compared to the exerted nodal forces in the problem should be small.

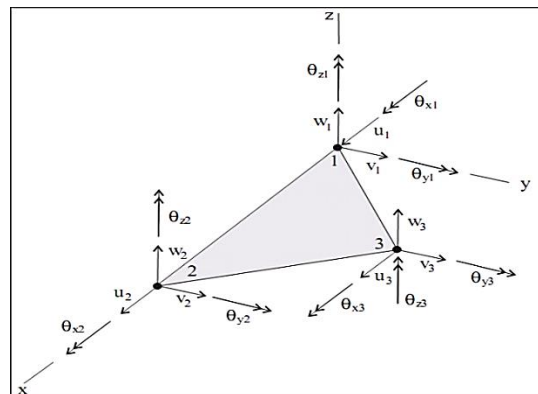


Figure 3. Shell structural element

2.4. MODEL OPTIMIZATION

In order to model the foundation and the slope, the dimensions of the sloped perimeter and the foundation layer situated underneath have been taken into consideration following the investigation of a number of models with different dimensions and increased distances of boundaries as well as by ignoring the influence of the boundaries. Two dimensions of the model were set as a constant value, and the third one as a variable to achieve suitable dimensions. Afterward, various values were

selected for the variable dimension, for each of which the model displacements at the slope toe were calculated. Figs 4-6 illustrate the diagrams of the outputs. For instance, in order to find the appropriate dimension in the x-axis direction, the dimensions in the y-axis and z-axis directions are assumed to be the constant values of 20m and 30m, and the maximum displacement for the models with the dimensions of 20, 40, 60 and 80 in the x-axis direction is recorded as shown in Fig. 4, respectively.

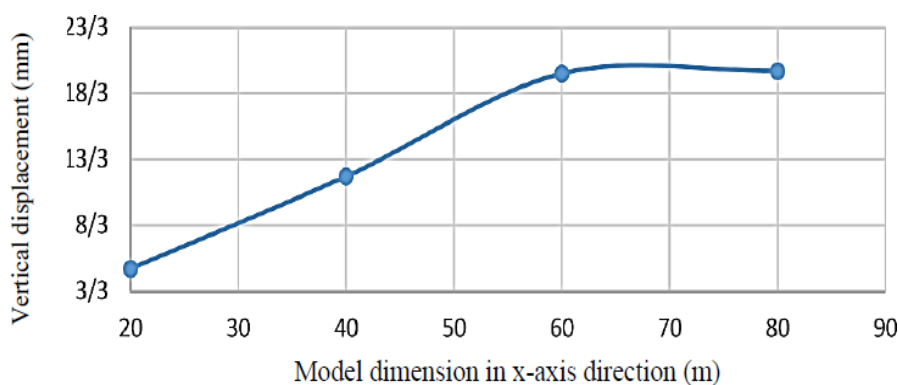


Figure 4. Vertical displacement of the model in terms of its dimensions in the x-axis direction.

As depicted in Fig. 4, the vertical displacement of the slope toe increases by moving the model boundaries forward in the x-axis direction, which virtually remains constant in the dimension domain of 60-80m. The trend of Fig. 4 shows that for the dimensions more than 60m, the magnitude of the model displacements will not

change, and hence it can be stated that the suitable dimension for the model in the x-axis direction is equal to 60m. Obviously, for the dimensions less than 20m, there are also variations in the vertical displacement. Similar to the x-axis, the relevant diagrams for the y-axis and z-axis are presented in Figs. 5 and 6, respectively.

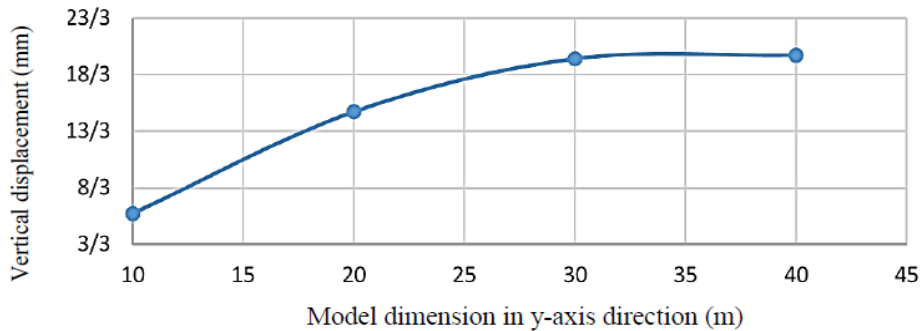


Figure 5. Vertical displacement of the model in terms of its dimensions in the y-axis direction.

The total number of the elements used in the model is equal to 26,354 zones, which has been chosen akin to the selection of the model dimensions in Fig. 7. In order to mesh the model, it has been attempted to utilize cubic elements (with identical edge scales) as these elements

will lead to the best result in the model. Furthermore, the mesh size in the location of the strip foundations, due to the more sensitivity of the loading conditions and high values of displacements, has been considered finer than that in other zones.

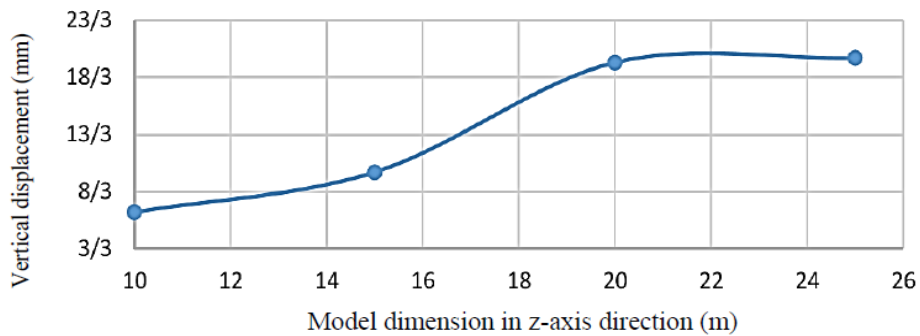


Figure 6. Vertical displacement of the model in terms of its dimensions in the z-axis direction.

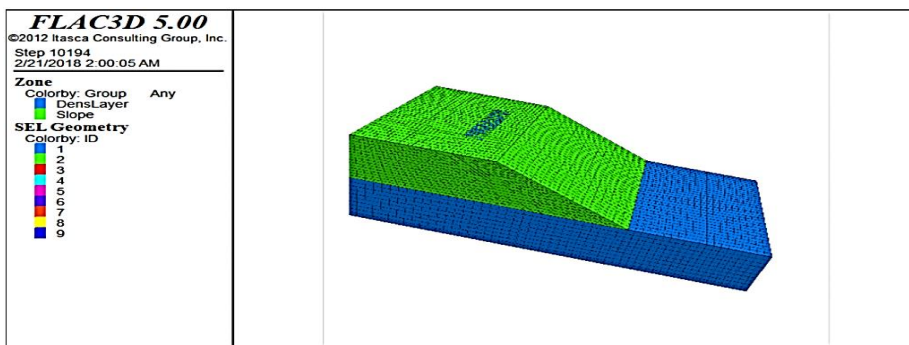


Figure 7. Developed model

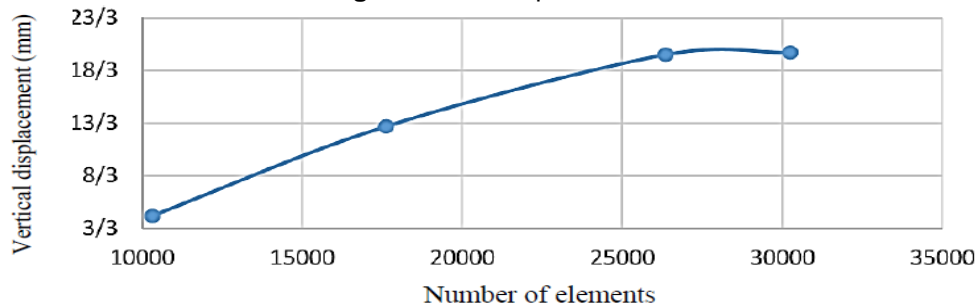


Figure 8. Vertical displacement of the model in terms of the number of the elements used in modeling

2.5. CHARACTERISTICS OF SOIL AND STRUCTURAL ELEMENTS

The properties considered for the soil slope and the layer of the foundation located beneath are represented in Table 1. As previously mentioned, the Mohr-Coulomb (MC)

constitutive model has been employed to model the soil of the foundation and of the slope.

Table 1. Soil properties

	Mass per unit volume (kg/m ³)	Internal friction angle	Cohesion (kPa)	Shear modulus (MPa)	Bulk modulus (MPa)
Foundation layer	2200	33	200	208	278
Soil slope	1950	31	10	27	42

The definite properties considered for the soil encompass density, bulk modulus and shear modulus, [Table 1](#). In addition, the probabilistic soil parameters include the

internal friction angle and cohesion, the statistical distribution of which has been tabulated in [Table 2](#).

Table 2. Properties of the probabilistic parameters considered for the soil

Mean cohesion (kPa)	Mean internal friction angle (degrees)	Cohesion standard deviation (kPa)	Standard deviation of internal friction angle (degrees)
10	31	5	5

Additionally, [Tables 3](#) and [4](#) present the characteristics of the geogrid and shell (strip foundation) elements, respectively. It should be noted that the cap of the isotope

has been taken into account, and the length-to-width ratio of the strip foundation as more than five.

Table 3. Characteristics of the geogrid element

Elasticity modulus (MPa)	Poisson's ratio	Coupling spring stiffness (cs_sk) (N/m)	coupling spring cohesion (cs_scoh) (kPa)	coupling spring friction (cs_sfric) (degrees)
4.14	0.33	7590	0	29.2

Table 4. Characteristics of the strip foundation element

Elasticity modulus (kPa)	Poisson's ratio	Cross-sectional dimension (mxm)	Cross section thickness (m)	Specific mass (kg/m3)
2.9x107	0.2	16x3	1.2	2400

3. RESULTS AND DISCUSSION

3.1. LOADING ON STRIP FOUNDATION

The shell element used has an elastic behavior. In this stage, the previous displacements, which have been due to bringing the model into a balanced state, are firstly

removed onto the foundation head. The exerted loading, in the static state, has been evaluated as 500 kN.

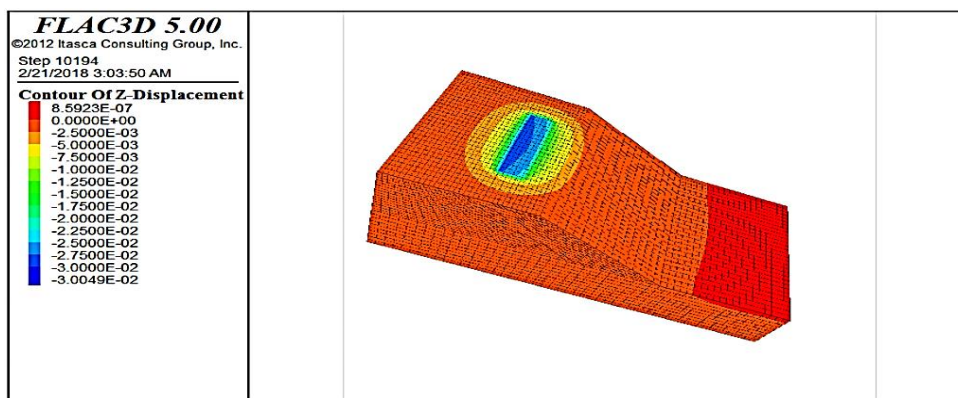


Figure 9. Vertical displacement following applying loading on foundation

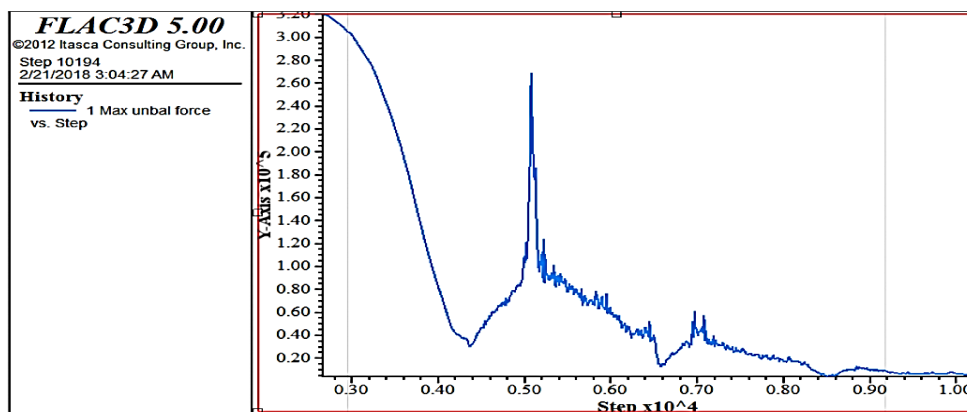


Figure 10. Graph of unbalanced force

As can be observed in [Fig. 10](#), despite having an ascending trend in some parts of the model, the unbalanced force has an overall descending trend until reaching the zero point in the diagram, which

demonstrates the suitable balance of the model following the loading imposed on the foundation. Moreover, as illustrated in [Figs. 11](#) and [12](#), the diagrams of the settlement and horizontal displacement in the model –

time histories of the settlement and horizontal displacement in a point with the coordination of

(20,15,20) – have ultimately reached a constant value, indicating the model balance.

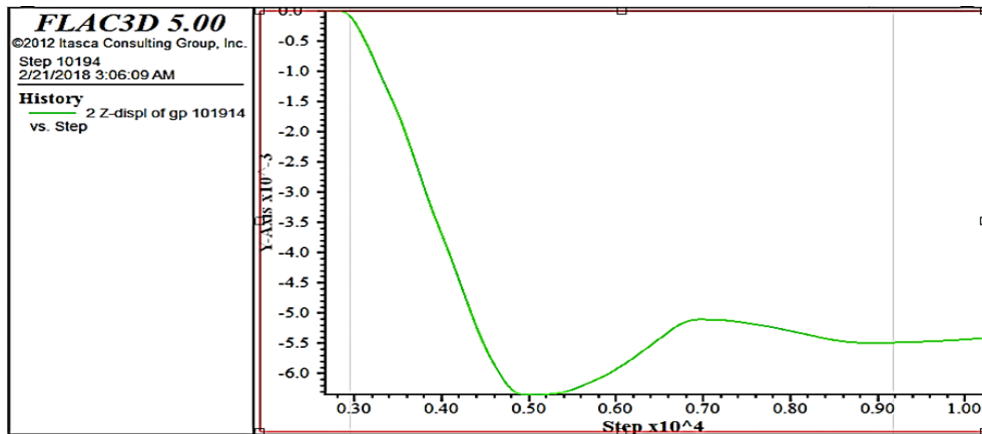


Figure 11. Diagram of model settlement

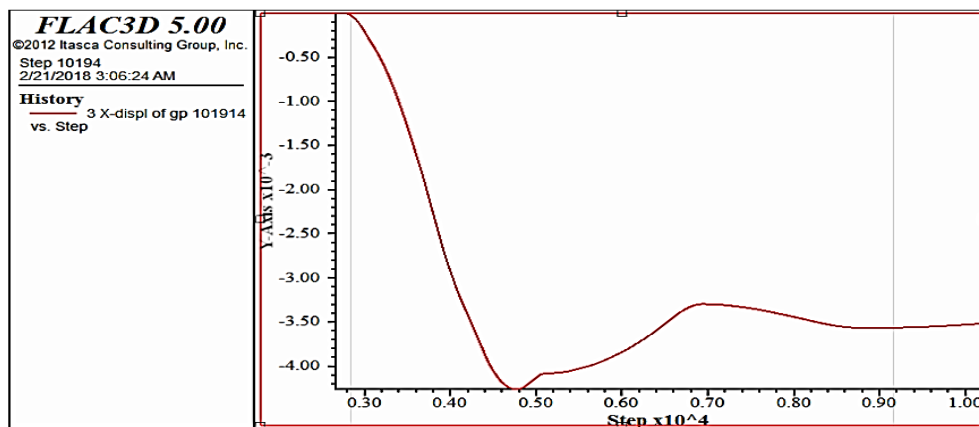


Figure 12. Diagram of model horizontal displacement

3.2. PROBABILISTIC ANALYSIS

Because of the indefiniteness and inherent variability of the physical and strength parameters of soils along with the measurement errors and approximations existing in analytic models, the slope stability analysis is a probabilistic phenomenon, in which a probabilistic distribution is obtained in terms of the variable input parameters. As a result, it is possible to calculate the probability of occurrence of different safety factors or the failure probability of the desired slope. Since designers are not comprehensively familiar with the probabilistic-analytic solution associated with the problems, the simple method of simulation will be very efficient to achieve the probabilistic solutions. In the Monte Carlo (MC)

simulation method, by stochastically sampling the probabilistic distribution of the input parameters calculated as well as by iterating the sampling, the relevant parameters can be evaluated, followed by the probabilistic distribution of the obtained results. Assuming a distribution similar to the normal distribution for the input parameters, it can be found that the probabilistic distribution is also symmetrical; and the mean and mode values are consistent with one another. The values calculated via the definite method, which have been evaluated by averaging the input data, are also compatible with the probabilistic distribution mean

3.3. INVESTIGATING THE BEARING CAPACITY BY A DEFINITE ANALYSIS

3.3.1. ASSESSMENT OF THE SLOPE ANGLE EFFECT

In order to investigate the effect of the slope angle, the four angles of 25, 35, 45 and 55 degrees have been considered in modeling. In these models, a foundation with the width of 3m and the length of 16m has been used. It should be noted that, in all these models, the foundation distance from the sloped boundary has been taken into

account as 4.5m, the dimensions of the geogrid sheet as two times the dimensions of the strip foundation, and the depth of the geogrid sheet as the half of the width of the strip foundation, i.e., 1.5m. Fig. 13 indicates the graph of the bearing capacity for the strip foundation for the slope with the angle of 55 degrees.

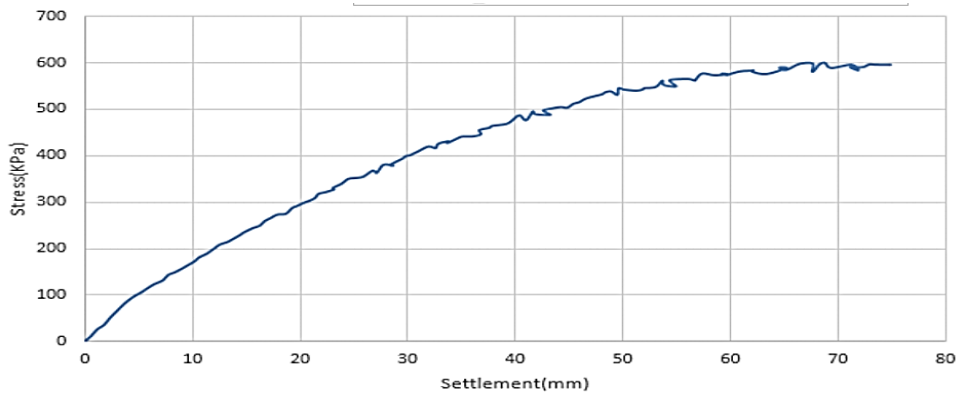


Figure 13. Bearing capacity of strip foundation for angle of 55 degrees

Referring to [Fig. 13](#), the bearing capacity in terms of the slope angle of 55 degrees is nearly equal to 600kPa, the corresponding settlement of which is 75mm. Obviously, the settlement of the strip foundation increases as the stress applied to the foundation increases. Initially, the gradient of these variations is relatively constant. In the case of higher stresses, however, the graph gradient decreases until it becomes horizontal. [Fig. 14](#) represents the graph of the strip foundation bearing capacity in terms of the angle of 45 degrees. According to [Fig. 14](#), the strip foundation bearing capacity in the case of the slope angle of 45 degrees is approximately 650kPa, and the corresponding settlement is 71mm. By reducing the slope

angle from 55 degrees to 45 degrees, the bearing capacity increases by virtually 8%. Increasing the slope angle will reduce the vertical displacement, the reason of which is the rise in the vertical component of the soil reaction in the soil-foundation interaction. The diagram of the strip foundation bearing capacity for the angle of 35 degrees is drawn in [Fig. 15](#), in which the strip foundation bearing capacity in the case of the slope angle of 35 degrees is almost 705kPa with the corresponding settlement of 76mm. As observed here, reducing the slope from 55 degrees to 35 degrees will lead to the increase of the strip foundation bearing capacity by 17%.

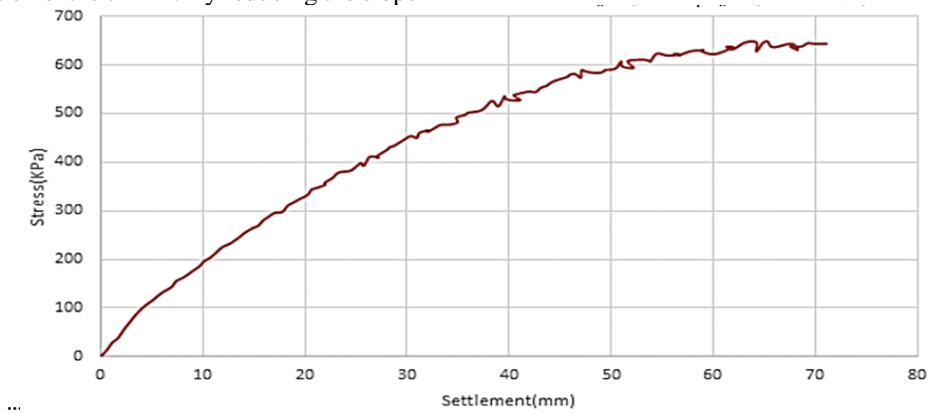


Figure 14. Bearing capacity of strip foundation for angle of 45 degrees

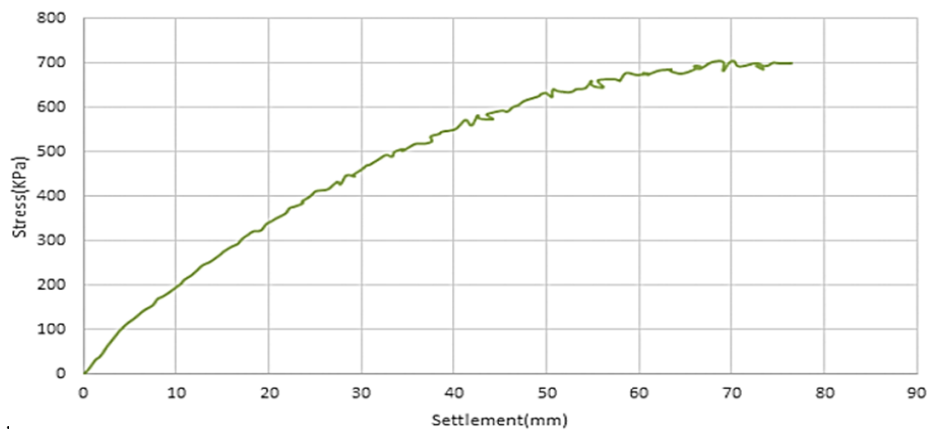


Figure 15. Bearing capacity of strip foundation for angle of 35 degrees

[Fig. 16](#) shows the strip foundation bearing capacity for the slope angle of 25 degrees, in which the bearing capacity and the corresponding settlement are 730kPa and 69mm, respectively. It can be found, by comparing the graph of

the bearing capacity in [Figs. 15](#) and [16](#), reducing the slope angle from 35 degrees to 25 degrees has increased the slope bearing capacity by nearly 4%.

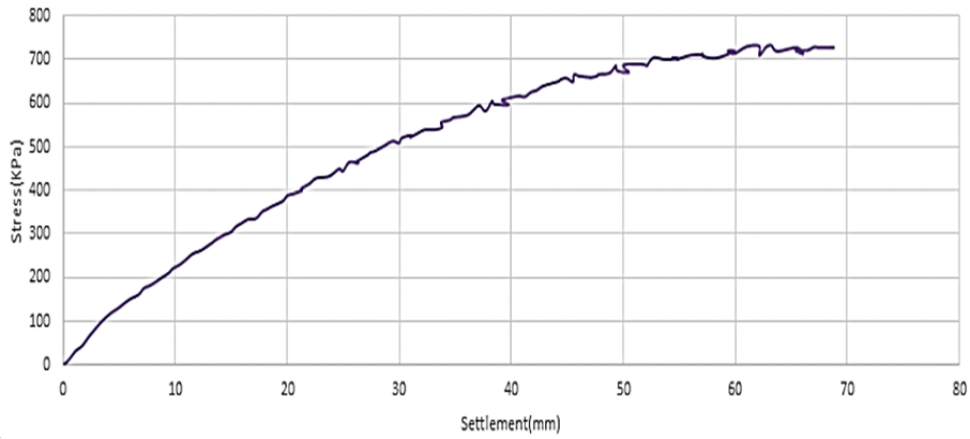


Figure 16. Bearing capacity of strip foundation for angle of 25 degrees

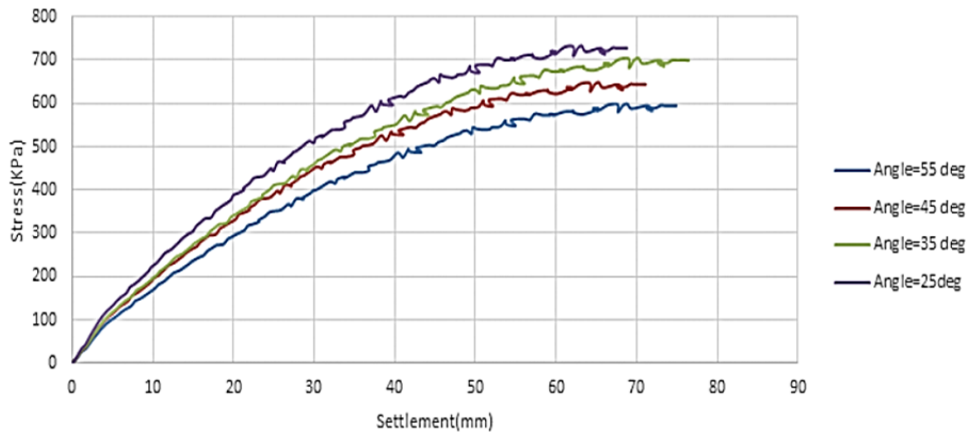


Figure 17. Bearing capacity of strip foundation in terms of different slope angles

The strip foundation bearing capacity in terms of different slope angles has been compared in Fig. 17. As depicted in Fig. 17, as the slope angle decreases from 55 degrees to 25 degrees (almost a two-time reduction), the strip foundation bearing capacity increases

from 600kPa to 730kPa, which is almost 22%. It should be mentioned that higher reductions in the slope angle will lead to less increases in the strip foundation bearing capacity.

3.4. INVESTIGATING THE BEARING CAPACITY BY PROBABILISTIC ANALYSIS

3.4.1. ASSESSMENT OF THE SLOPE ANGLE EFFECT

In order to investigate the effect of the slope angle in the probabilistic analyses, similar to the previous (definite) method, the four angles of 25, 35, 45 and 55 degrees have been considered in modeling. In these models, a 16m (L) × 3m (W) foundation has been used. It should be stated that, in all these models, the foundation distance from the sloped boundary has been chosen as 4.5m, the dimensions

of the geogrid sheet as two times the dimensions of the strip foundation, and the depth of the geogrid sheet as the half of the width of the strip foundation, i.e., 1.5m. Fig. 18 illustrates the comparison among the normal distributions of the strip foundation bearing capacity in terms of different slope angles.

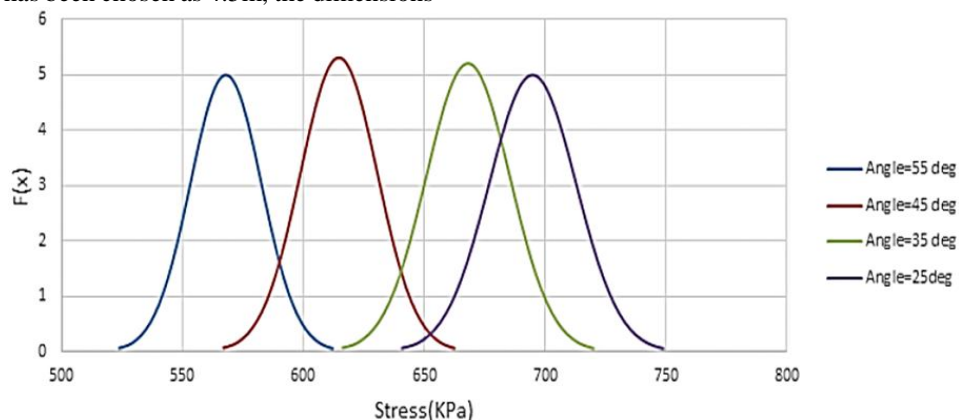


Figure 18. Normal distribution of strip foundation bearing capacity in terms of different slope angles

As shown in Fig. 18, in the case of the probabilistic analysis, a decrease in the slope angle from 55 degrees to

25 degrees (an approximate two-time reduction) increases the mean of the strip foundation bearing capacity in the

normal distribution in the form of an increase by 21%, from 570kPa to 695kPa. Comparing the outputs of the bearing capacity in the definite analysis method to those

of the mean bearing capacity in the normal distribution, it can be concluded that the bearing capacity of the strip foundation will diminish in the latter case.

4. CONCLUSION

With the reduction in the slope, from 55 degrees to 25 degrees (almost a two-time drop), the strip foundation bearing capacity increases from 600kPa to 730kPa (by virtually 22%). However, the more the slope angle decreases, the less the strip foundation bearing capacity will increase. In the case of the probabilistic analysis, reducing the slope angle from 55 degrees to 25 degrees (an approximate two-time decrease) results in increasing

The mean of the bearing capacity of the strip foundation from 570kPa to 695kPa (by almost 21%) in the normal distribution. Based on the comparison of the results of the bearing capacity between the definite analysis method and the mean bearing capacity in the normal distribution method, it can be established that the bearing capacity of the strip foundation will decrease in the mean probabilistic analysis method.

FUNDING/SUPPORT

Not mentioned any Funding/Support by authors.

AUTHORS CONTRIBUTION

This work was carried out in collaboration among all authors.

ACKNOWLEDGMENT

Not mentioned by authors.

CONFLICT OF INTEREST

The author (s) declared no potential conflicts of interests with respect to the authorship and/or publication of this paper

5. REFERENCES

- [1] Todd MK. Handbook of geotechnical investigation and design tables. 2nd ed. Australia: CRC Press; 2017 Jun 29. [\[View at Google Scholar\]](#); [\[View at Publisher\]](#).
- [2] Carroll MM, Katsube N. The role of Terzaghi effective stress in linearly elastic deformation. 1983 Dec 1; 105(4): 509-511. [\[View at Google Scholar\]](#); [\[View at Publisher\]](#).
- [3] Filz GM. Load transfer, settlement, and stability of embankments founded on columns installed by deep mixing methods. National Technical University of Athens School of Civil Engineering Geotechnical Department–Foundation Engineering Laboratory. 2007; [1-35](#). [\[View at Google Scholar\]](#); [\[View at Publisher\]](#).
- [4] Tafreshi SM, Dawson AR. Comparison of bearing capacity of a strip footing on sand with geocell and with planar forms of geotextile reinforcement. Geotextiles and Geomembranes. 2010 Feb 1;28(1):72-84. [\[View at Google Scholar\]](#); [\[View at Publisher\]](#).
- [5] Altalhe EB, Taha MR, Abdrabbo FM. Bearing capacity of strip footing on sand slopes reinforced with geotextile and soil nails. Jurnal Teknolog. 2013 Sep 25;65(2):1-11. [\[View at Google Scholar\]](#); [\[View at Publisher\]](#).
- [6] Han J, Gabr MA. Numerical analysis of geosynthetic-reinforced and pile-supported earth platforms over soft soil. Journal of geotechnical and geoenvironmental engineering. 2002 Jan;128(1):44-53. [\[View at Google Scholar\]](#); [\[View at Publisher\]](#).
- [7] Ye GB, Wang M, Zhang Z, Han J, Xu C. Geosynthetic-reinforced pile-supported embankments with caps in a triangular pattern over soft clay. Geotextiles and Geomembranes. 2020 Feb 1;48(1):52-61. [\[View at Google Scholar\]](#); [\[View at Publisher\]](#).
- [8] Girout R, Blanc M, Thorel L, Dias D. Geosynthetic reinforcement of pile-supported embankments. Geosynthetics International. 2018 Jan 8;25(1):37-49. [\[View at Google Scholar\]](#); [\[View at Publisher\]](#).
- [9] Shams B, Ardakani A, Roustaei M. Laboratory investigation of geotextile position on CBR of clayey sand soil under freeze-thaw cycle. Scientia Iranica. 2019 Jan 23;1(1): 1-31. [\[View at Google Scholar\]](#); [\[View at Publisher\]](#).
- [10] Pokharel SK, Han J, Leshchinsky D, Parsons RL. Experimental evaluation of geocell-reinforced bases under repeated loading. International Journal of Pavement Research and Technology. 2018 Mar 1;11(2):114-127. [\[View at Google Scholar\]](#); [\[View at Publisher\]](#).
- [11] Satyal SR, Leshchinsky B, Han J, Neupane M. Use of cellular confinement for improved railway performance on soft subgrades. Geotextiles and Geomembranes. 2018 Apr 1;46 (2):190-205. [\[View at Google Scholar\]](#); [\[View at Publisher\]](#).
- [12] Tingle JS. Mechanistic Analyses of Geosynthetic Reinforced Aggregate Road Test Sections. Transportation Research Record. 2019 Sep 15; 2673(12): 1-15. [\[View at Google Scholar\]](#); [\[View at Publisher\]](#).
- [13] Goodman RE. Karl Terzaghi: The engineer as artist. United States of America: American Society of Civil Engineers; 1999. [\[View at Google Scholar\]](#); [\[View at Publisher\]](#).
- [14] Hull JH, inventor; AquaBlok Ltd, assignee. Soil-like material and method of making a barrier for containing waste. United States patent application US 16/090,882. 2019 Oct 31. [\[View at Google Scholar\]](#); [\[View at Publisher\]](#).
- [15] Huang B, Gong H, Shu X. Evaluation of Geosynthetics Reinforcement in Flexible Pavement Structures Using Accelerated Pavement Testing. Nashville: TDOT; 2018 Oct. TN 37243. [\[View at Google Scholar\]](#); [\[View at Publisher\]](#).
- [16] Malkawi AI, Hassan WF, Abdulla FA. Uncertainty and reliability analysis applied to slope stability. Structural safety. 2000 Jun 1;22(2):161-187. [\[View at Google Scholar\]](#); [\[View at Publisher\]](#).

- [17] Esfandiari J, Selamat MR. Laboratory investigation on the effect of transverse member on pull out capacity of metal strip reinforcement in sand. *Geotextiles and Geomembranes*. 2012 Dec 1;35:41-49. [\[View at Google Scholar\]](#); [\[View at Publisher\]](#).
- [18] Liu M, Yang M, Wang H. Bearing behavior of wide-shallow bucket foundation for offshore wind turbines in drained silty sand. *Ocean Engineering*. 2014 May 15; 82:169-179. [\[View at Google Scholar\]](#); [\[View at Publisher\]](#).
- [19] Charlton TS, Rouainia M. A probabilistic approach to the ultimate capacity of skirted foundations in spatially variable clay. *Structural Safety*. 2017 Mar 1;65:126-136. [\[View at Google Scholar\]](#); [\[View at Publisher\]](#).
- [20] Li L, Li J, Huang J, Liu H, Cassidy MJ. The bearing capacity of spudcan foundations under combined loading in spatially variable soils. *Engineering geology*. 2017 Sep 21;227:139-148. [\[View at Google Scholar\]](#); [\[View at Publisher\]](#).
- [21] Park JS, Park D. Vertical bearing capacity of bucket foundation in sand overlying clay. *Ocean Engineering*. 2017 Apr 1;134:62-76. [\[View at Google Scholar\]](#); [\[View at Publisher\]](#).
- [22] Hegde A, Sitharam TG. 3-Dimensional numerical modelling of geotextile reinforced sand beds. *Geotextiles and Geomembranes*. 2015 Apr 1;43(2):171-181. [\[View at Google Scholar\]](#); [\[View at Publisher\]](#).
- [23] Cerato AB, Lutenecker AJ. Scale effects of shallow foundation bearing capacity on granular material. *Journal of Geotechnical and Geoenvironmental Engineering*. 2007 Oct;133(10):1192-1202. [\[View at Google Scholar\]](#); [\[View at Publisher\]](#).
- [24] Naseri, F., Bagherzadeh Khalkhali, A. Evaluation of Seismic Performance of Concrete Gravity Dams Under Soil-structure-reservoir Interaction Exposed to Vertical Component of Near-field Earthquakes During Impounding Case study: Pine Flat Dam. *Journal of civil Engineering and Materials Application*, 2018; 2(4): 181-191. [\[View at Google Scholar\]](#); [\[View at Publisher\]](#).